Mon. Not. R. Astron. Soc. **000**, 1–4 (2011) Printed 18 January 2012 (MN LATEX style file v2.2)

The origin of cosmic-ray electrons in cluster outskirts

Anders Pinzke[1⋆], Peng Oh[1⋆], and Christoph Pfrommer[2⋆]
[1]*University of California - Santa Barbara, Department of Physics, CA 93106-9530, USA*
[2]*Heidelberg Institute for Theoretical Studies (HITS), Schloss-Wolfsbrunnenweg 33, DE - 69118 Heidelberg, Germany*

18 January 2012

ABSTRACT
bla bla bla

Key words: magnetic fields, cosmic rays, radiation mechanisms: non-thermal, elementary particles, galaxies: cluster: general

1 INTRODUCTION

2 SIMULATIONS

Our simulations were performed in a ΛCDM universe using the cosmological parameters: $\Omega_\mathrm{m} = \Omega_\mathrm{DM} + \Omega_\mathrm{b} = 0.3$, $\Omega_\mathrm{b} = 0.039$, $\Omega_\Lambda = 0.7$, $h = 0.7$, $n_\mathrm{s} = 1$, and $\sigma_8 = 0.9$. The total matter density in units of the critical density of the universe ρ_crit is denoted by Ω_m, the baryonic density by Ω_b, the DM density by Ω_DM and the cosmological constant today is denoted by Ω_Λ. The critical density, $\rho_\mathrm{crit} = 3H_0/(8\pi G)$, where the present day Hubble constant $H_0 = 100\,h\,\mathrm{km\,s^{-1}\,Mpc^{-1}}$. n_s represents the spectral index of the primordial power-spectrum, and σ_8 denotes the *rms* linear mass fluctuation within a sphere of radius $8\,h^{-1}$Mpc extrapolated to $z = 0$. The simulations were carried out with an updated and extended version of the distributed-memory parallel TreeSPH code GADGET-2 (Springel 2005; Springel et al. 2001). Gravitational forces were computed using a combination of particle-mesh and tree algorithms. Hydrodynamic forces are computed with a variant of the smoothed particle hydrodynamics (SPH) algorithm that conserves energy and entropy where appropriate, i.e. outside of shocked regions (Springel & Hernquist 2002). Our simulations follow the radiative cooling of the gas, star formation, supernova feedback, and a photo-ionizing background (details can be found in Pfrommer et al. 2007). We model the cosmic ray (CR) physics in a self-consistent way (Pfrommer et al. 2006; Enßlin et al. 2007; Jubelgas et al. 2008). We include the adiabatic CR transport process such as compression and rarefaction, and a number of physical source and sink terms which modify the cosmic ray pressure of each CR population separately. The most important sources considered for injection are, diffusive shock acceleration at cosmological structure formation shocks and shock waves in supernova remnants, while the primary sinks are thermalization by Coulomb interactions, and catastrophic losses by hadronization. For simplicity, in this paper we do not take into account CRs injected into the inter-stellar medium from supernova remnants (see Pinzke, Oh, and Pfrommer, in prep. for a discussion of this topic).

⋆ e-mail:apinzke@physics.ucsb.edu (AP); peng@physics.ucsb.edu (PO);pfrommer@h-its.org (CP)

2.1 CR protons

The CR proton distribution function is given by

$$f_\mathrm{p}(p_\mathrm{p}) = \frac{\mathrm{d}^2 N_\mathrm{p}}{\mathrm{d}p_\mathrm{p}\,\mathrm{d}V} = C\,p_\mathrm{p}^{-\alpha}\,\theta(p_\mathrm{p} - q)\,, \tag{1}$$

and $p_\mathrm{p} = P_\mathrm{p}/m_\mathrm{p}c$, where we have normalized the proton momentum P_p with the proton mass m_p. Here q is the normalized momentum cutoff, α the spectral index, and C the normalization in units of density.

From our simulated galaxy clusters we derive for each snapshot at time t the injected CR proton distribution function f_p. We select particles in the outskirts of clusters where the gas densities are low and hence the Coulomb cooling of the CR protons small. The CR proton distribution function from the simulations is parameterized in terms of adiabatic invariant momentum cutoff q_0 and the adiabatic invariant Lagrangian amplitude of the spectrum $\tilde{C}_0$. We convert the adiabatic invariant quantities to physical quantities through

$$q = \left(\frac{\rho}{\rho_0}\right)^{\frac{1}{3}} q_0\,, \tag{2}$$

and

$$\tilde{C} = \left(\frac{\rho}{\rho_0}\right)^{-\frac{\alpha-1}{3}} \tilde{C}_0\,, \tag{3}$$

where the convenient unitless redefinition of the CR proton amplitude is given by

$$\tilde{C} = C\,m_\mathrm{p}/\rho\,. \tag{4}$$

The injected distribution function is calculated as the change in normalization between each snapshot, $f_\mathrm{inj,p}(p_\mathrm{p}) = \Delta C\,p_\mathrm{p}^{-\alpha}$, and is derived through the formalism developed in Enßlin et al. (2007) and Jubelgas et al. (2008):

$$\begin{aligned}\Delta C(t+\Delta t) &= C(t)\frac{\Delta\varepsilon_\mathrm{CR}(t) - T_\mathrm{p}(q(t))\,\Delta n_\mathrm{CR}(t)}{\varepsilon_\mathrm{CR}(t) - T_\mathrm{p}(q(t))\,n_\mathrm{CR}(t)}\,, \quad \text{where}\\ \Delta X(t) &= X(t+\Delta t) - X(t)\,.\end{aligned} \tag{5}$$

We fix the time between each snapshot Δt to 100 Myrs, which is smaller then the loss timescale of CR electrons in cluster outskirts. The CR proton number density is given by

$$n_{\rm CR} = \int_0^\infty {\rm d}p_{\rm p}\, f_{\rm p}(p_{\rm p}) = \frac{C\, q^{1-\alpha}}{\alpha - 1}\,, \tag{6}$$

provided $\alpha > 1$. The kinetic energy density of the CR proton population is

$$\begin{aligned}\varepsilon_{\rm CR} &= \int_0^\infty {\rm d}p_{\rm p}\, f_{\rm p}(p_{\rm p})\, T_{\rm p}(p_{\rm p}) = \frac{C\, m_{\rm p}\, c^2}{\alpha - 1} \times \\ &\left[\frac{1}{2}\, {\rm B}_{\frac{1}{1+q^2}}\left(\frac{\alpha-2}{2}, \frac{3-\alpha}{2}\right) + q^{1-\alpha}\left(\sqrt{1+q^2} - 1\right)\right], \end{aligned} \tag{7}$$

where $T_{\rm p}(p_{\rm p}) = (\sqrt{1+p_{\rm p}^2} - 1)\, m_{\rm p}\, c^2$ is the kinetic energy of a CR proton. ${\rm B}_x(a,b)$ denotes the incomplete Beta-function, and $\alpha > 2$ is assumed.

3 RADIO RELICS

RELICS... Collisionless cluster shocks are able to accelerate ions and electrons in the high-energy tail of their Maxwellian distribution functions through diffusive shock acceleration (for reviews see Drury 1983; Blandford & Eichler 1987; Malkov & O'C Drury 2001). Neglecting non-linear shock acceleration and cosmic ray modified shock structure, then electrons and protons are indistinguishable in the process of diffusive shock acceleration. There are, however, difference in: (1) the maximum energy of the steady state spectrum that depends on the details of the shock, (2) acceleration efficiency that is related to the smaller Larmor radius of the electrons that keeps the electrons from diffusing back and forth over the discontinuity of the shock front.CHECK

In this section we derive the CR electron distribution function by rescaling the injected CR proton spectrum to account for the different acceleration efficiencies as well as the shift in momentum due to the factor ~ 2000 difference in mass. In addition we model the Coulomb and radiative losses of the CR electrons.

3.1 CR electron distribution function

In a hot plasma the temperatures of electrons and protons (ions) are equal. Under this constraint we derive the relationship between CR electron momentum and CR proton momentum given by

$$\begin{aligned} {\rm d}p_{\rm e} &= {\rm d}p_{\rm p}\, g(p_{\rm e}) = {\rm d}p_{\rm p}\, h(p_{\rm p})\,, \qquad \text{where} && (8)\\ g(p_{\rm e}) &= X\, \frac{\left[p_{\rm e}^2 - 2\,(X-1)\left(1 - \sqrt{1+p_{\rm e}^2}\right)\right]^{0.5}}{p_{\rm e} + (X-1)\,\dfrac{p_{\rm e}}{\sqrt{1+p_{\rm e}^2}}}\,, \qquad \text{and} && (9)\\ h(p_{\rm p}) &= X\, \frac{p_{\rm p} - (1-Y)\,\dfrac{p_{\rm p}}{\sqrt{1+p_{\rm p}^2}}}{\left[p_{\rm p}^2 + 2\,(1-Y)\left(1 - \sqrt{1+p_{\rm p}^2}\right)\right]^{0.5}}\,. && (10)\end{aligned}$$

(11)

Note that $p_{\rm e} = {\rm P}_{\rm e}/m_{\rm e}c$ and $p_{\rm p} = {\rm P}_{\rm p}/m_{\rm p}c$, where we have normalized the electron momentum $\rm P_e$ and the proton momentum $\rm P_p$ with the electron mass $m_{\rm e}$ and proton mass $m_{\rm p}$, respectively. We have introduced the mass ratios $X = m_{\rm p}/m_{\rm e}$ and $Y = m_{\rm e}/m_{\rm p}$. Also note that ${\rm dP_e} \rightarrow {\rm dP_p}$ in the asymptotic limit where $p_{\rm p} \gg 1$, and that ${\rm dP_e} \rightarrow \sqrt{m_{\rm e}/m_{\rm p}}\,{\rm dP_p}$ for $p_{\rm p} \ll 1$.

The injected CR electron distribution function at each time t is given by

$$\begin{aligned} f_{\rm inj,e}(p_{\rm e}) &= \frac{{\rm d}^2 N_{\rm inj,e}}{{\rm d}V{\rm d}p_{\rm e}}(p_{\rm e}) = \frac{{\rm d}^2 N_{\rm inj,e}}{{\rm d}V{\rm d}p_{\rm p}}(p_{\rm e})\frac{1}{g(p_{\rm e})} \\ &= \frac{{\rm d}^2 N_{\rm inj,p}}{{\rm d}V{\rm d}p_{\rm p}}(p_{\rm p})\left(\frac{p_{\rm e}}{p_{\rm p}}\right)^{-\alpha}\frac{\eta_{\rm max,e}}{\eta_{\rm max,p}}\frac{1}{g(p_{\rm e})} = \Delta C\, p_{\rm e}^{-\alpha}\frac{\eta_{\rm max,e}}{\eta_{\rm max,p}}\frac{1}{g(p_{\rm e})}\,. \end{aligned} \tag{12}$$

We use that maximal 50% of the energy available in a shock is injected into CR protons ($\eta_{\rm max,p}$) and a factor 10 smaller efficiency of 5% for the CR electrons ($\eta_{\rm max,e}$).

The CR electrons cool through inverse Compton (IC) emission and Coulomb losses on timescales that are relative short compared to the dynamical timescale of a cluster. We model these looses analytically by instantiniuosly injecting a power-law of electrons at time t_i and evolving it to a later time t (for further details see (Sarazin 1999)). The loss of energy for each particle is described by

$$\frac{{\rm d}\gamma}{{\rm d}t} = -b(\gamma, t)\,, \tag{13}$$

where the loss function $b(\gamma, t)$ is dominated by Coulomb and IC losses for the energies and gas densities relevant in this work. The Coulomb losses are given by

$$\begin{aligned} b_{\rm C}(\gamma) &= b_{\rm C}\gamma^2 = \frac{3\,\sigma_{\rm T}\, n_{\rm el}\, c}{2}\left[\ln\left(\frac{m_{\rm e}c^2\sqrt{\gamma-1}}{\hbar\,\omega_{\rm plasma}}\right)\right. \\ &- \left.\ln(2)\left(\frac{1}{2} + \frac{1}{\gamma}\right) + \frac{1}{2} + \left(\frac{\gamma-1}{4\gamma}\right)^2\right]. \end{aligned} \tag{14}$$

Here $\omega_{\rm plasma} = \sqrt{4\pi e^2 n_{\rm e}/m_{\rm e}}$ is the plasma frequency, and $n_{\rm e}$ is the number density of free electrons. Since the Coulomb losses for relativistic electrons is almost independent of energy (logarithmic), we approximate that $b_{\rm C}(\gamma, t) \approx b_{\rm C}(t)$ [1]. We can now derive the shift in energy γ_i at time t_i to energy γ at time t due to Coulomb cooling by integrating Eqn. (13):

$$\gamma_{\rm low} \equiv \int_{t_i}^{t} {\rm d}t\, b_{\rm C}(t) = -\int_{\gamma_i}^{\gamma} {\rm d}\gamma' = -(\gamma - \gamma_i)\,. \tag{15}$$

Since we have discrete snapshots in time we can approximate

$$\gamma_{\rm low} = \Delta t \sum_j b_{\rm C}(t_j)\,, \tag{16}$$

where the sum includes all snapshots from time t_i to time t. We now continue with the IC losses that are given by

$$b_{\rm IC}(\gamma, z) = b_{\rm IC}\gamma^2(1+z)^4 = \frac{4}{3}\frac{\sigma_{\rm T}}{m_{\rm e}c}U_{\rm cmb}\gamma^2\,. \tag{17}$$

Here $\sigma_{\rm T} = 8\pi e^4/3(m_{\rm e}c^2)^2$ is the Thomson cross section and $U_{\rm cmb}$ is the energy density of the CMB at redshift $z = 0$. Similarly to the Coulomb cooling we derive the evolution of energy of a particle subject to IC losses through

$$\frac{{\rm d}\gamma}{\gamma^2} = -b_{\rm IC}(1+z)^4{\rm d}t\,. \tag{18}$$

After a time $(t - t_i)$ has elapsed, all the electrons with energies above $\gamma_{\rm max}$ have thermalized, where we derive $\gamma_{\rm max}$ through integrating Eqn. (18) from injected time $z_i = z(t_i)$ to a later time $z = z(t)$:

[1] We use a constant energy $\gamma = 10^2$ to model the very weak dependence of energy, and note that the particular value of γ does not matter as long as $\gamma \gg 1$.

$$\frac{1}{\gamma_{\rm max}} \equiv \frac{1}{\gamma} - \frac{1}{\gamma_i} = \frac{b_{\rm IC}}{H_0}\left[\Lambda(z) - \Lambda(z_i)\right] . \quad (19)$$

Here $\Lambda(z) \approx z + 1.23\,z^2 + 0.50\,z^3 - 0.14\,z^4 - 0.04\,z^5$ in a Lambda CDM universe and $H_0 = h\,{\rm km\,s^{-1}\,Mpc^{-1}}$ is the Hubble constant.

Given an initial energy γ_i of an electron at time t_i, Eqn. (13) can be integrated to give the value of γ at a later time t. The differential population density for relativistic electrons ($\gamma_{\rm e} \approx p_{\rm e} = P_{\rm e}/m_{\rm e}c$) is then given by

$$f_{\rm inj,e}(\gamma, t, t_i) = f_{\rm inj,e}(\gamma_i, t_i)\left.\frac{\partial\gamma_i}{\partial\gamma}\right|_t , \quad \text{where} \quad (20)$$

$$f_{\rm inj,e}(\gamma_i, t_i) = f_{\rm inj,e}(\gamma - \Delta\gamma_{\rm IC} - \Delta\gamma_{\rm C}, t_i)$$

$$= f_{\rm inj,e}(\gamma + \frac{\gamma^2}{\gamma_{\rm max} - \gamma} + \gamma_{\rm low}, t_i) , \quad \text{and} \quad (21)$$

$$\frac{\partial\gamma_i}{\partial\gamma} = \frac{\gamma_{\rm max}^2}{(\gamma_{\rm max} - \gamma)^2} . \quad (22)$$

Here we have used that $\Delta\gamma_{\rm IC} = -\gamma_{\rm low}$ and $\Delta\gamma_{\rm C} = \frac{-\gamma^2}{\gamma_{\rm max}-\gamma}$. The total electron spectrum is derived from the sum of all individually cooled injected spectra, starting from the time of injection t_i until a later time t,

$$f_{\rm tot,e}(\gamma, t) = \left(\frac{\tilde{\rho}_{gas}(t)}{\rho_0}\right)^{-1/3} \sum_j f_{\rm inj,e}(\gamma, t, t_j) . \quad (23)$$

Here the comoving gas density factor $\rho_{gas}(t)$ takes care of the adiabatic gains and losses, where $\rho_0 = 1$ is a reference density in GADGET. Also note that the electrons injected at time $t = t_i$ have not had the time to cool yet.

We model the final CR electron spectrum as a superposition of five CR populations, each determined by Eqn. 23 but with a different spectral index and injected spectra.

3.2 Synchrotron emission

The process of merging clusters is often very violent where large amounts of gravitational energy being dissipated in the form of radiation, increased temperature, turbulence flows and shocks. The two latter processes are believed to accelerate CRs to high energy, where especially the distribution function of preexisting CRs is enhanced. In this section we use the smooth CR electron distribution derived from a simulated merging cluster in the previous section, boost it using the details of the shock, and then finally derive the radio synchrotron emission.

We fit the steady state CR electron distribution function in Fig. **??** with two power-laws

$$f_{\rm e,fit}(\gamma_{\rm e}) = C_1\,\gamma_{\rm e}^{-\alpha_1}\theta(\gamma_{\rm break} - \gamma_{\rm e}) + C_2\,\gamma_{\rm e}^{-\alpha_2}\theta(\gamma_{\rm e} - \gamma_{\rm break}) . \quad (24)$$

The best fit CR electron normalization is given by $\mathbf{C} = (6 \times 10^{-4}, 10^7)$, the spectral index by $\alpha = (3.0, 5.5)$, and the energy where the slope changes by $\gamma_{\rm break} = 1.2 \times 10^4$.

Probably need to calculate the emissivity numerically since there is a break in the power-law spectrum. CHECK We calculate the radio synchrotron emissivity of the CR electrons using Rybicki & Lightman (1979)

$$J_0(\nu) \approx \left(\frac{e^2\,\nu_c}{c}\right)\sum_i C_i\gamma\left(\frac{3\alpha_i - 1}{12}\right)\gamma\left(\frac{3\alpha_i + 19}{12}\right)\frac{3^{\frac{\alpha_i}{2}}}{\alpha_i + 1}\left(\frac{\nu}{\nu_c}\right)^{\frac{1-\alpha}{2}} , \quad (25)$$

where the cyclotron frequency is given by $\nu_c = e\,B\,c/(2\pi m_{\rm e}c^2)$. We derive the total emitted power from the source by integrating the emissivity over the target volume. Here, we assume that the target volume haw an uniform distribution of the CR electrons, hence the total power per unit frequency is given by

$$P_0(\nu) = {\rm Volume} \times J_0(\nu) . \quad (26)$$

NEED TO REWRITE The typical size of a large relic is of the order of a Mpc, while the thickness is only of the order 100 kpc. We assume that the rather unknown extension of the relic along the line of sight to be about 500 kpc, where the total radio emitting volume is about 0.05 Mpc^3. In addition we assume that the average magnetic field in the cluster outskirts to be of the order $B \approx 0.1\,\mu$G. The total emitted power at 1.4 PHz of the size typical for a large radio Relic is then given by $P_0(1.4\,{\rm PHz}) = 9 \times 10^{22}$ W/Hz. This is about a factor 10-100 smaller than what is typically expected from a relic van Weeren et al. (2009). However, this luminosity is boosted by the shock or turbulence induced during a cluster merger. We follow the prescription outlined in Kang & Ryu (2011) to calculate the boost in radio luminosity due to reacceleration, and find that $P_2(1.4\,{\rm PHz}) \sim \times 10^{25}$ W/Hz in agreement with several of the relics listed in e.g. van Weeren et al. (2009).

The steady-state test-particle solution of the downstream CR distribution can be written as a function of the pre-existing CRs through

$$f_2(\gamma_{\rm e}) = q\gamma_{\rm e}^{-q}\int_{\gamma_{\rm inj}}^{\gamma}\gamma'^{q-1}f_{\rm e,fit}(\gamma'){\rm d}\gamma' . \quad (27)$$

Here we have neglected the contribution from the injected CRs. The lowest momentum boundary above which particles can cross the shock is given by

$$\gamma_{\rm inj} \approx 1.17\frac{u_2}{c}\left(1 + \frac{1.07}{\epsilon_B}\right)\left(\frac{M}{3}\right)^{0.1} . \quad (28)$$

Spectral index

$$q(M) = \frac{3\,(u_1 - v_A)}{u_1 - v_A - u_2} = \frac{3\sigma\left(1 - M_A^{-1}\right)}{\sigma - 1 - \sigma M_A^{-1}} \quad (29)$$

where u_1 and u_2 are the speed of the flow upstream and downstream, respectively, in the shock rest frame. The compression ratio is given by $\sigma = u_1/u_2 = \rho_2/\rho_1$, and $M_A = u_1/v_A$ is the upstream Alfvn Mach number with velocity $v_A = B_1/\sqrt{4\pi\rho_1}$. We derive the test-particle power-law slope q as a function of the shock Mach number M with $\sigma = [(\gamma_{\rm ad} + 1)M^2]/[(\gamma_{\rm ad} - 1)M^2 + 2]$, where adiabatic index $\gamma_{\rm ad} = 5/3$, $M_A = Mc_s/v_A$, and c_s the upstream sound speed.

Enhanced emissivity calculated with

$$\frac{J_2(\nu)}{J_0(\nu)} \approx \left(\frac{B_2^{(r-1)/2}}{B_0^{(\alpha-1)/2}}\right)\left[\frac{f_2(\gamma_{\rm e})}{f_0(\gamma_{\rm e})}\right]_{\gamma_{\rm e}=10^4}\left(\frac{\nu}{280\,{\rm MHz}}\right)^{(\alpha-r)/2} . \quad (30)$$

OUTLINE THE PRESCRIPTION eq7, eq21

4 CONCLUSIONS

ACKNOWLEDGMENTS

REFERENCES

Blandford R., Eichler D., 1987, Phys. Rep., 154, 1
Drury L. O., 1983, Reports of Progress in Physics, 46, 973
Enßlin T. A., Pfrommer C., Springel V., Jubelgas M., 2007, A&A, 473, 41
Jubelgas M., Springel V., Enßlin T., Pfrommer C., 2008, A&A, 481, 33

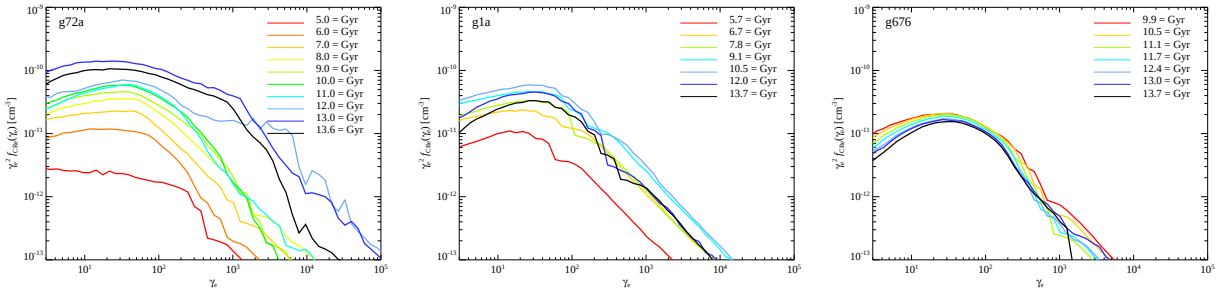

Figure 1. Time evolution of the cosmic ray electron spectra in cluster outskirts. We show the total volume weighted CR electron distribution function for the particles that reside end up in region between (1.3-1.5)R_{200} at redshift zero; a cluster with a recent merger (g72a, left panel), large cooling flow cluster (g1a, middle panel), and a small cooling flow cluster (g676, right panel). The different line colors show the CR electron spectra at different look-back times, where the most recent spectrum in black is at 13.6 Gyrs. Notice the larger scatter in the merging cluster, and the relative small difference in the cooling flow clusters. The shape of the distribution function is very similar between different cooling flow clusters, and slightly more stochastic for merging clusters.

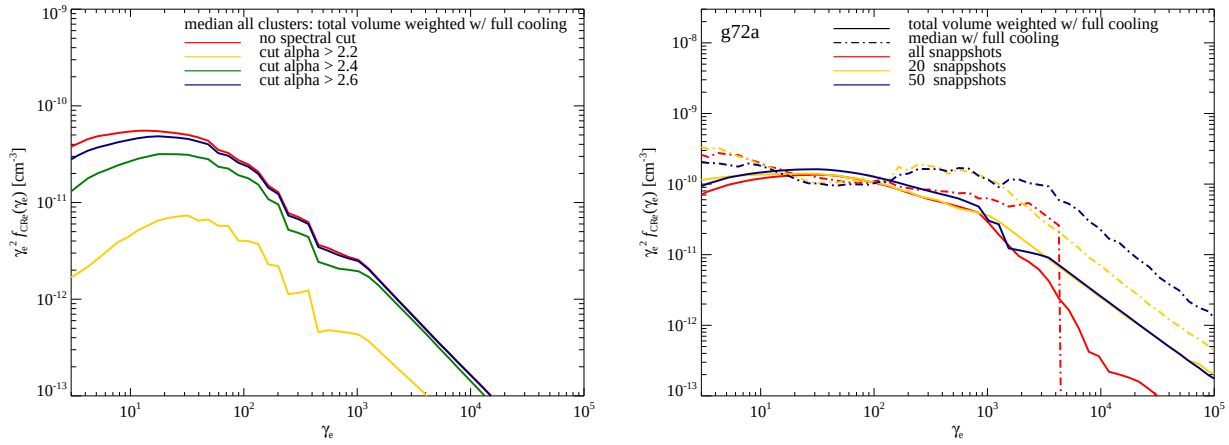

Figure 2. Testing the robustness of the CR electron spectra. Left panel shows how different cuts in injected spectra impact the total volume weighted CR electron spectrum with full cooling; no spectral cut (red line), cut particles with $\alpha_{\rm inj} > 2.2$ (yellow line), cut particles with $\alpha_{\rm inj} > 2.4$ (green line), cut particles with $\alpha_{\rm inj} > 2.6$ (blue line). Note that in the main CR model we cut all particles with an $\alpha_{\rm inj} > 2.4$, which is a factor four smaller at low energies than the spectrum without a cut. Right panel shows the effect of time-resolution on the CR electron spectra. The median CR spectrum is shown with full cooling that includes radiative, Coulomb, and adiabatic losses (dash-dotted line), the solid line represents the total volume weighted CR electron spectrum with full cooling. The three line colors corresponds to the same cluster, a large coma like merging cluster, but with different time resolution between snapshots in the relevant regime; red lines corresponds to 100 Myrs between snapshots, orange lines corresponds to (1.0-1.5) Gyrs between snapshots, and the blue lines corresponds to (1.0-1.5) Gyrs between snapshots.

Kang H., Ryu D., 2011, ApJ, 734, 18

Malkov M. A., O'C Drury L., 2001, Reports of Progress in Physics, 64, 429

Pfrommer C., Enßlin T. A., Springel V., Jubelgas M., Dolag K., 2007, MNRAS, 378, 385

Pfrommer C., Springel V., Enßlin T. A., Jubelgas M., 2006, MNRAS, 367, 113

Rybicki G. B., Lightman A. P., 1979, Radiative processes in astrophysics. New York, Wiley-Interscience

Sarazin C. L., 1999, ApJ, 520, 529

Springel V., 2005, MNRAS, 364, 1105

Springel V., Hernquist L., 2002, MNRAS, 333, 649

Springel V., Yoshida N., White S. D. M., 2001, New Astronomy, 6, 79

van Weeren R. J., Röttgering H. J. A., Brüggen M., Cohen A., 2009, A&A, 508, 75

This paper has been typeset from a TEX/ LATEX file prepared by the author.

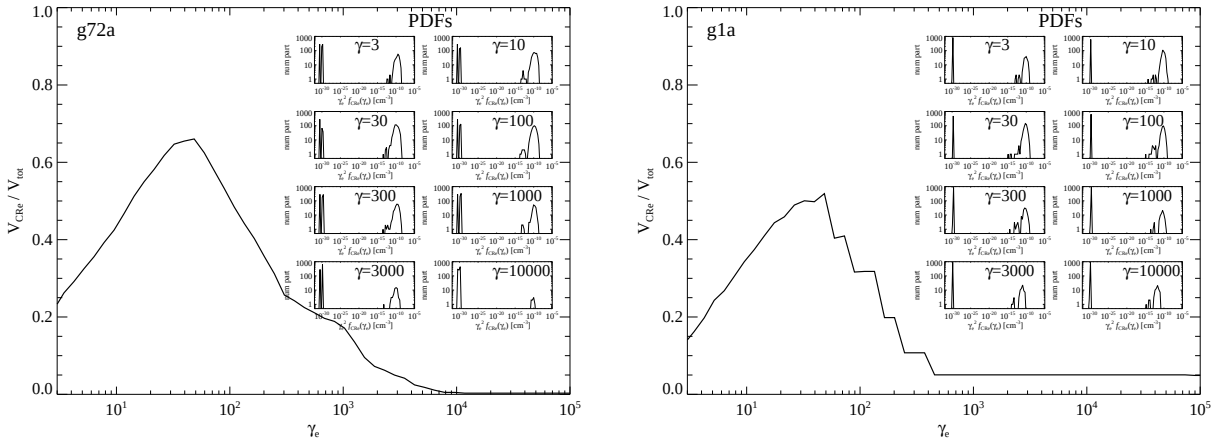

Figure 3. The fractional volume occupied by CR electrons in cluster outskirts. Large panels (left Coma like cluster, and right massive cooling flow cluster) show the fractional volume occupied by CR electrons as a function of logarithmic Lorentz factor (γ_e) in the region between (1.3-1.5)R_{200} at redshift zero. The smaller panels show the logarithmic particle distribution function for different γ_e, where the left peaks corresponds to unpopulated SPH particles and cooled CR particles, while the right peaks show the CR populated SPH particles.

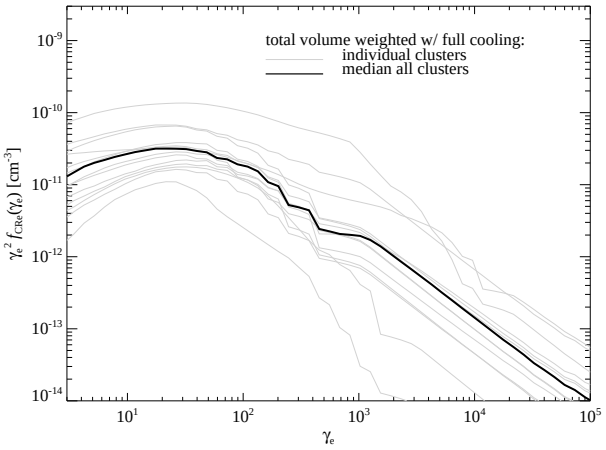

Figure 4. Cosmic ray electron spectra in cluster outskirts at redshift zero. We show the total volume weighted CR electron distribution function in the region between (1.3-1.5)R_{200} with full cooling that includes radiative, Coulomb, and adiabatic losses. The the thin grey lines show the spectra from individual clusters while the thick solid line shows the median of the spectra from all clusters.

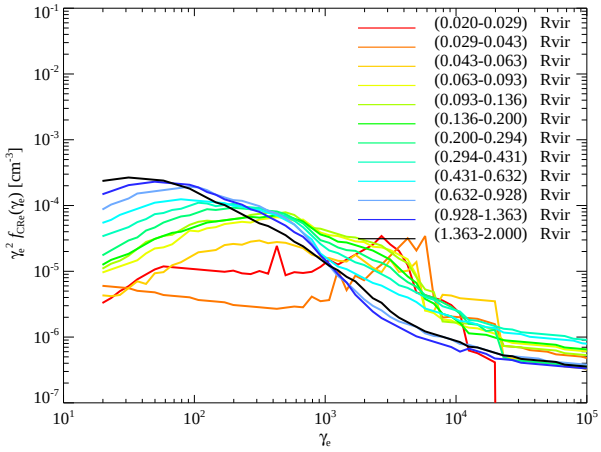

Figure 5. Spatial dependence of the cosmic ray electron spectra at redshift zero. We show the total volume weighted CR electron distribution function; a Coma like cluster (left panel), a massive cooling flow cluster (middle panel), and the median of our 14 cluster's spectra (right panel). The different line colors show the CR electron spectra for different radial bins.

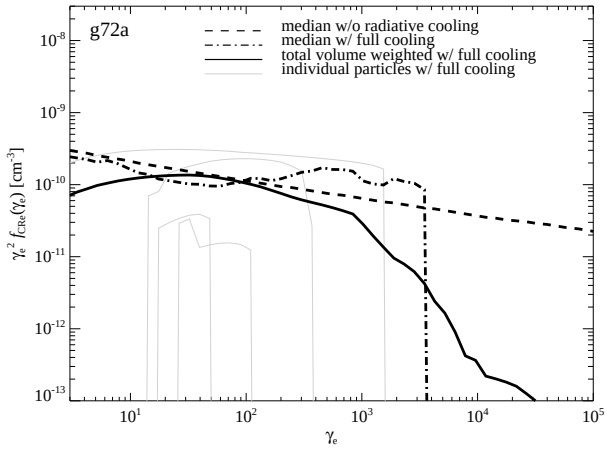

Figure 6. Cosmic ray electron spectra in cluster outskirts at redshift zero. We show the CR electron distribution function weighted with the electron Lorentz factor (γ_e) squared for a typical cluster with a recent merger for region between (1.3-1.5)R_{200}. The median CR spectrum is shown with full cooling that includes radiative, Coulomb, and adiabatic losses (dash-dotted line), and with only adiabatic losses (dashed line). The solid line represents the total volume weighted CR electron spectrum with full cooling. Note that the Coulomb cooling at low energies is very inefficient because of the low electron densities in the cluster outskirts.